Distribution Network Topology Detection with Time-Series Measurements

G. Cavraro
DEI - University of Padova
Padova, Italy
cavraro@dei.unipd.it

R. Arghandeh
CIEE - U. C. Berkeley
Berkeley, USA
arghandeh@berkeley.edu

G. Barchi
DISI - University of Trento
Trento, Italy
grazia.barchi@unitn.it

A. von Meier
EECS - U.C. Berkeley
Berkeley, USA
vonmeier@berkeley.edu

***Abstract*—This paper proposes a novel approach to detecting the topology of distribution networks based on the analysis of time series measurements. The analysis approach draws on data from high-precision phasor measurement units (PMUs or synchrophasors) for distribution systems. A key fact is that time-series data taken from a dynamic system show specific patterns regarding state transitions such as opening or closing switches, as a kind of signature from each topology change. The algorithm proposed here is based on the comparison of the actual signature of a recent state transition against a library of signatures derived from topology simulations. The IEEE 33-bus model is used for initial algorithm validation.**

I. Introduction

Power transmission networks tend to be far better equipped with measurement devices than distribution systems, for economic reasons and necessity. For transmission systems, the ratio of available measurements to state variables ranges from about 1.7 to 2.2 in practice, meaning that the operating state of the system is generally observable [1]. Distribution systems, by contrast, are largely unobservable beyond the substation. Switches and protective devices may not reliably communicate their status to the distribution operator, so the topology can only be determined with certainty on location, by sending crews into the field. With the integration of distributed energy resources (DER), electric vehicles and controllable loads, the need for observability in distribution systems is increasing. Along with impacts on voltage levels, DER will affect faults or short circuits both upstream and downstream in the feeder. Reconfiguration actions may be more frequent, the risk of unintentional islands may be greater, and the actual topology status of the system may be less clear. But knowledge of the correct, updated topology is essential for safety, for service restoration after outages, and for any advanced operating strategies such as volt-VAR optimization [2], [3]. Different tools have been developed and implemented to monitor distribution network behavior with more detailed and timely information, such as SCADA (supervisory control and data acquisition), smart meters and line sensors. Creating situational awareness out of disjointed data streams still remains a challenge, though. Given the present monitoring technologies, more, better and faster data from behind the substation will be needed to realize smart distribution networks [4]. The cost of monitoring systems in distribution networks remains a barrier to equipping all nodes with measurement devices. To some extent, a capable Distribution System State Estimation (DSSE) can compensate for the lack of direct sensor data to support observability. However, switch status errors will easily be misinterpreted as analog measurement errors (e.g. voltage or current readings). Thus topology detection is an important enabling technology for state estimation as well as a host of other functions based on knowledge of the system operating state in real-time.

Previous work on distribution network topology detection tackles the problem from different perspectives. In [5] authors propose a state estimation algorithm that incorporates switching device status as additional state variables. A normalized residual test is used to identify the best estimate of the topology. In the typical radial topologies of distribution circuits, opening of a switching device results in some lost loads downstream. The analysis of expected load values performed by aggregating and mapping multiple loads to a common switching device (such as a sectionalizer, circuit breaker, fuse or recloser) suspected of being open. In [6], the authors provide a tool for choosing sensor placement for topology detection. Given a particular placement of sensors, the tool reveals the confidence level at which the status of switching devices can be detected. Authors in [7] and [8] are focused on estimating the impedance at the feeder level. However, even a perfect identification of network impedance cannot always guarantee the correct topology, since multiple topologies could present very similar impedances.

In this paper, a novel approach to topology detection is proposed based on time series analysis of measurements. This approach is inspired by high-precision phasor measurement units (PMUs or synchrophasors) for distribution systems, which the authors are involved in implementing [9]. The main idea derives from the fact that time-series data from a dynamic system show specific patterns regarding system state transitions, a kind of signature left from each topology change. The algorithm is based on the comparison of the actual signature of a switching action and a library of signatures derived from simulations of different topology transitions. We build a trend matrix and a trend vector from system observations in order to understand when the topology change occurred, and to identify the new topology.

The rest of this paper is organized as follows: Section II describes the distribution network model. Section III describes how switching actions will propagate in the mathematical representation. Section IV presents our topology detection algorithm, and Section V shows the initial validation through simulation in a 33-bus system.

II. Distribution Network Model and Physical Topology

This section presents the distribution network model and its related notations. Given a matrix W, we denote its (element-wise) complex conjugate by $\bar{W}$, its transpose by W^T and

978-1-4799-1785-3/15/$31.00 ©2015 IEEE

its conjugate transpose by W^*. We denote the real and the imaginary part of W by $\Re(W)$ and by $\Im(W)$, respectively. We denote the entry of W that belongs to the j-th row and to the k-th column by $[W]_{jk}$. We define the column vector of all ones by $\mathbf{1}$. Given two vectors v and w, we denote by $\langle v, w\rangle$ the inner product v^*w. We associate the electric grid with a directed graph $\mathcal{G} = (\mathcal{V}, \mathcal{E}, \sigma, \tau)$, where $\mathcal{V}$ is the set of nodes (the buses), $\mathcal{E}$ is the set of edges (the electrical lines connecting them). Moreover $\sigma, \tau : \mathcal{E} \to \mathcal{V}$ are two functions such that edge $e \in \mathcal{E}$ goes from the source node $\sigma(e)$ to the terminal node $\tau(e)$. Finally, with $\boldsymbol{T}_j$ we define the j-th possible topology.

In this study, we assume that the system reaches its steady-state condition after a switching action and all voltages and currents are sinusoidal signals with the same frequency ω_0. Thus, they can be expressed via a complex number whose magnitude corresponds to the signal root-mean-square value, and whose phase corresponds to the phase of the signal with respect to an arbitrary global reference. Therefore, x represents the signal $x(t) = |x|\sqrt{2}\sin(\omega_0 t + \angle x)$. The system state is described by the following quantities:

- $u \in \mathbb{C}^n$, where u_v is the grid voltage at node v;
- $i \in \mathbb{C}^n$, where i_v is the current injected at node v;
- $s = p + iq \in \mathbb{C}^r$, where s_v, p_v and q_v are the complex, the active and the reactive power injected at node v.

We model the substation as an ideal sinusoidal voltage source (*slack bus*) at the distribution network nominal voltage U_N, with arbitrary, but fixed, angle ϕ. We also consider, without loss of generality, $\phi = 0$. We model all nodes but the substation as *constant power* or *P-Q buses*. It is known that the system state satisfies the following equations

$$i = \boldsymbol{Y} u \tag{1}$$
$$u_0 = U_N \tag{2}$$
$$u_v i_v = p_v + iq_v \qquad v \neq 0 \tag{3}$$

$\boldsymbol{Y}$ is the bus admittance matrix of the grid, defined as

$$[\boldsymbol{Y}]_{jk} = \begin{cases} \sum_{j \neq k} y_{jk}, & \text{if } j = k \\ -y_{jk}, & \text{otherwise} \end{cases} \tag{4}$$

where y_{jk} is the admittance of the branch connecting bus j and bus k and where we neglect the shunt admittances. From (4) we have

$$\boldsymbol{Y}\mathbf{1} = 0 \tag{5}$$

and then $\mathbf{1}$ (all-ones vector) belongs to the Kernel of $\boldsymbol{Y}$. Furthermore, it can be shown that if $\mathcal{G}$, the graph associated to the electrical grid, is connected, then the kernel of $\boldsymbol{Y}$ has dimension 1.

The following Lemma [10] introduces a particular pseudo inverse of $\boldsymbol{Y}$, which will be useful in the proposed algorithm proof.

Lemma 1: There exists a unique symmetric, positive semidefinite matrix $\boldsymbol{X} \in \mathbb{C}^{n \times n}$ such that

$$\begin{cases} \boldsymbol{X}\boldsymbol{Y} = I - \mathbf{1}\mathbf{1}_0^T \\ \boldsymbol{X}\mathbf{1}_0 = 0. \end{cases} \tag{6}$$

The matrix $\boldsymbol{X}$ is related to the Moonre Penrose pseudoinverse $\boldsymbol{X}^P$ of $\boldsymbol{Y}$ by the equation

$$\boldsymbol{X} = (I - e_0\mathbf{1}^T)\boldsymbol{X}^P \tag{7}$$

Applying Lemma 1, from (1) we can express voltages of the grid as a function of currents

$$u = \boldsymbol{X} i + \mathbf{1}U_N \tag{8}$$

Finally, we introduce the useful approximation of the relationship between voltages and powers [10], that is basically a first order Taylor expansion w.r.t. the nominal voltage U_N.

Proposition 2: Consider the physical model described by the set of nonlinear equations (1), (2), (3) and (8). Node voltages then satisfy

$$u = U_N\mathbf{1} + \frac{1}{U_N}\boldsymbol{X}\bar{s} + o\left(\frac{1}{U_N}\right) \tag{9}$$

(the little-o notation means that $\lim_{U_N \to \infty} \frac{o(f(U_N))}{f(U_N)} = 0$).

Power flow equations are highly non-linear. In the presence of measurement noise and load uncertainty in distribution networks, finding the power flow solution can be numerically intensive. The former proposition is a linear approximation of power flow equations. It is applied to state estimation [11], Volt/Var optimization [3], and the optimal power flow problem [12].

III. Identification of Switching Actions

In this section we discuss how topology changes appear in the network representation. The basic idea behind our proposed approach is that changes in switching status will create specific signatures in the grid measurands (voltage, current, frequency, etc) that allow us to infer what is happened. In order to develop the theoretical base for the proposed algorithm and its ease of mathematical proof, we make two assumptions. However, these assumptions will be relaxed in Section V, thus the algorithm will be tested in a more realistic condition.

Assumption 3: We assume that the loads are not time varying at the time of switching action.

Assumption 4: We assume that all the lines have the same resistance over reactance ratio. Therefore, $\Im(y_e) = \alpha\Re(y_e), \forall e \in \mathcal{E}$, where y_e is the admittance of the line e. This assumption is used for ease of admittance matrix decomposition.

Now assume that at time $t-1$ before the switches status changes, the distribution network has the topology $\boldsymbol{T}_j$ with bus admittance matrix $\boldsymbol{Y}_j$. Because of Assumption 4 and because $\boldsymbol{Y}_j$ is symmetric, $\Im(\boldsymbol{Y}_j)$ and $\Re(\boldsymbol{Y}_j)$ share the same eigenvector. Therefore, we can write

$$\boldsymbol{Y}_j = U\Sigma_R U^* + iU\Sigma_I U^* \tag{10}$$

where Σ_R, Σ_I are diagonal matrices whose diagonal entries are the non-zero eigenvalues of $\Im(\boldsymbol{Y}_j)$ and $\Re(\boldsymbol{Y}_j)$, and U is an orthonormal matrix that includes all the associated eigenvector. Furthermore, Assumption 4 allows us to write $\Sigma_I = \alpha\Sigma_R$. Utilizing the well known properties of the Moore Penrose pseudoinverse and (7), we have

$$\begin{aligned} \boldsymbol{X}_j &= (I - e_0\mathbf{1}^T)\left(U(\Sigma_R)^{-1}U^* - i\alpha U(\Sigma_R)^{-1}U^*\right) \\ &= (I - e_0\mathbf{1}^T)\boldsymbol{X}_j^P \end{aligned} \tag{11}$$

and thus, applying Proposition 2 and neglecting the infinitesimal term, the voltages can be expressed as

$$u(t-1) = \boldsymbol{X}_j\frac{\bar{s}}{U_N} + \mathbf{1}U_N \tag{12}$$

Now assume that at time t a switch, located in the edge e' change its status. After this action the new topology is $\boldsymbol{T}_k$. Since we are basically adding or deleting an edge from the graph that represents the grid, we can write

$$\boldsymbol{Y}_k = \boldsymbol{Y}_j + \gamma y_{e'} a_{e'} a_{e'}^T \tag{13}$$

where γ is $+1$ or -1 depending on whether the switch in e' is closing or opening, $y_{e'}$ is the admittance of the line e', and the elements of $a_{e'}$ are all zeroes except for $\sigma(e')$ and $\tau(e')$ for which is equal to $+1$ or -1 respectively. This allows us to write

$$u(t) = \boldsymbol{X}_k \frac{\bar{s}}{U_N} + \mathbf{1} U_N \tag{14}$$

It is now trivial from (5), U spans the image of $I - \mathbf{1}\mathbf{1}^T/(\mathbf{1}^T\mathbf{1})$, i.e. all $\mathbb{R}^n$ "except" $\mathbf{1}$. Since $a_{e'}$ is orthogonal to $\mathbf{1}$, there exists $b_{e'}$ such that $U b_{e'} = a_{e'}$. This allow us to write

$$\begin{aligned} \boldsymbol{Y}_k &= U(\Sigma_R + \Re(y_{e'}) b_{e'} b_{e'}^T) U^* + iU(\alpha \Sigma_R + \Im(y_{e'}) b_{e'} b_{e'}^T) U^* \\ \boldsymbol{X}_k &= (I - e_0 \mathbf{1}^T) \boldsymbol{X}_k^P \end{aligned} \tag{15}$$

where

$$\boldsymbol{X}_k^P = U(\Sigma_R + \Re(y_{e'}) b_{e'} b_{e'}^T)^{-1} U^* - iU(\alpha \Sigma_R + \Im(y_{e'}) b_{e'} b_{e'}^T)^{-1} U^* \tag{16}$$

Define the *trend vector* $\delta(t) = u(t) - u(t-1)$. Its properties will be fully exploited by our detection algorithm. We have, from (11) and (15),

$$\delta(t) = (I - e_0 \mathbf{1}^T) \Phi_{jk} \frac{\bar{s}}{U_N} \tag{17}$$

where $\Phi_{jk} = \boldsymbol{X}_k^P - \boldsymbol{X}_j^P$. The following Proposition is fundamental for the development of our topology detection algorithm.

Proposition 5: Φ_{jk} is a rank one matrix.

Proof: From (11), (15), using Ken Miller Lemma [13] with some simple computations, we can write

$$\Phi_{jk} = \left(\Re(y_e) - i \frac{\Im(y_e)}{\alpha^2} \right) U \Sigma_R^{-1} b_e b_e^T \Sigma_R^{-1} U^* \tag{18}$$

It's trivial to see that Φ_{jk} is a rank one matrix with normalized eigenvector

$$g_{jk} = \frac{U \Sigma_R^{-1} b_e}{\| U \Sigma_R^{-1} b_e \|} \tag{19}$$

associated to the non-zero eigenvalue

$$\lambda_{jk} = \left(\Re(y_e) - \frac{i}{\alpha^2} \Im(y_e) \right) \| U \Sigma_R^{-1} b_e \|^2 \tag{20}$$

We can therefore write $\Phi_{jk} = \lambda_{jk} g_{jk} g_{jk}^*$ That is, all the information included in a rank one matrix is contained in its non-zero eigenvalue and its associated eigenvector. ■

Thanks to Proposition 5, we can see that $\delta(t)$ represents how the opening or the closing of a switch spreads on the voltages profile, and it is spanned, Φ_{jk} being a rank one matrix, by $(I - e_0 \mathbf{1}^T) g_{jk}$, that is

$$\delta(t) \propto (I - e_0 \mathbf{1}^T) g_{jk}. \tag{21}$$

Therefore, every specific topology change has its associated normalized eigenvector g_{jk}, which is linearly related to the trend vector built from the time series measurements. This means every abrupt change in voltage measurement vector due to a switching action is linearly proportional to g_{jk}, that can be seen as its particular signature. This fact is the cornerstone for the topology detection algorithm in this paper. It means that network topology changes from $\boldsymbol{T}_j$ to $\boldsymbol{T}_k$ can be inferred directly from the Φ_{jk}, irrespective of other variables such as voltages u and loads s that describe the network operating state at the time.

IV. Proposed Topology Detection Algorithm

In Section III, we showed how each switching action can be inferred from the voltage measurement in the network and how it is fully characterized by the eigenvector introduced in (19). Assuming the distribution network physical infrastructure, i.e. conductor impedances and switch locations, are known, we can construct a topology library $\mathcal{L}$ in which we collect all the normalized eigenvectors (19) for all possible transitions from one topology to another (as a consequence of Proposition 5).

$$\mathcal{L} = \{ g_{jk} : \text{transition from } \boldsymbol{T}_j \text{ to } \boldsymbol{T}_k \text{ is possible} \} \tag{22}$$

In reality, there is some noise associated with PMUs or ant other type of measurement. The PMU measurements are presented by the complex vector y. The trend vector is also affected by the measurement noise. With a modification on notation, we denote the trend vector as the *empirical trend vector*

$$\delta(t) = y(t) - y(t-1) \tag{23}$$

The empirical trend vector analogous to the trend vector. After a topology change, we compare δ to the vectors in the topology library $\mathcal{L}$ in order to understand which topology transition happened. The comparison is made simply by projecting the normalized empirical trend vector $\frac{\delta}{\|\delta\|}$ onto the topology library $\mathcal{L}$. The projection is performed with the inner product, and it allows us to obtain for each vector in $\mathcal{L}$

$$c_{jk} = \left\| \left\langle \frac{\delta}{\|\delta\|}, (I - e_0 \mathbf{1}^T) g_{jk} \right\rangle \right\|, \tag{24}$$

If $c_{jk} \simeq 1$, it means that δ is spanned by $(I - e_0 \mathbf{1}^T) g_{jk}$ and the transition from $\boldsymbol{T}_j$ to $\boldsymbol{T}_k$ has occurred.

In actual distribution networks, loads are time varying. Therefore, the trend vector δ is typically non-zero even if there has not been any switching action. Thus we need a criterion that allows us to distinguish load-based variation of δ from switching actions. When a switch opens, a branch is deleted form the network graph. If a switch closes, a branch is added to the network. When any switch is opened or closed, there is usually an abrupt change in the currents flowing through some conductors, which cause abrupt voltages variation. Therefore, we need to distinguish normal behavior of sources and loads on the grid, and where the variation is due to a dramatic event like a topology change. We have been inspired by [14], in which the authors analyzed the maximum singular value (i.e. the norm) of a measurement history matrix for capturing major cyber attacks on measurement data. The measurement history matrix, here called the *trend matrix*, depends on the parameter w that is the size of the considered time window exploited for the computation of the trend matrix.

$$\Delta(t) = \begin{bmatrix} (y(t) - y(t-1))^T \\ \vdots \\ (y(t) - y(t-w))^T \end{bmatrix} \tag{25}$$

The parameter w must be tuned adequately. In Section V, there is a brief discussion on the selection of w. Notice that the

transpose of the trend vector composes the first row of the trend matrix. We compute the norm of Δ and when delta exceeds a chosen threshold, we state that there has been an abrupt change in the network topology and we perform the projection of the trend vector δ in the topology library. These considerations lead to the formalization of our topology detection algorithm as follows:

Algorithm 1 Topology transition detection

At each time t

1: PMUs at each node j record (noisy) voltage phasor measurements $y_j(t)$
2: the algorithm builds the trend vector $\delta(t)$ and the trend matrix $\Delta(t)$
3: **if** there is a significant spike in $\|\Delta(t)\|$ **then**
4: the algorithm projects $\delta(t)$ in $\mathcal{L}$ obtaining the set of values

$$\mathcal{C} = \left\{ c_{jk} = \left\| \left\langle \frac{\delta}{\|\delta\|}, (I - e_0 \mathbf{1}^T) g_{jk} \right\rangle \right\|, g_{jk} \in \mathcal{L} \right\};$$

5: the algorithm chooses the maximum in $\mathcal{C}$ and infer which switch has changed its status.
6: **end if**

V. Results, Discussions and Conclusions

We tested our algorithm for topology detection on the IEEE 33-bus distribution test feeder [15], which is illustrated in the Figure 1. In this testbed, there are five switches (namely S_1, S_2, S_3, S_4, S_5) that can be opened or closed, thus leading to the set of 32 possible topologies $\boldsymbol{T}_1, \ldots, \boldsymbol{T}_{32}$. Because of the ratio between the number of buses and the number of switches, some very similar topologies can occur (for example the topology where only S_1 is closed and the one in which only S_2 is closed). In the IEEE33-bus test case, Assumption 4 about line impedances does not hold, making the test condition somewhat more realistic than our initial presentation. For now, we assumed the distribution level PMUs are installed on every bus 267 every bus (this assumption will need to be revisited in light of economics). The algorithm has been tested in several

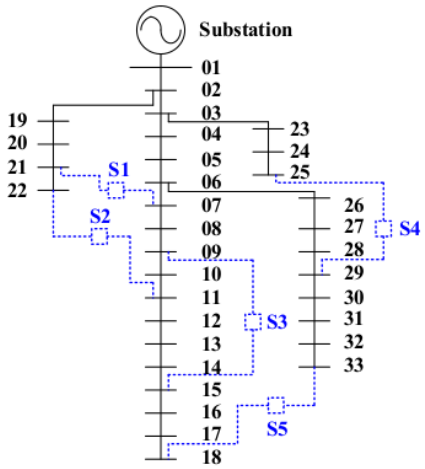

Figure 1. Schematic representation of the IEEE33 buses distribution test case with the five switches

scenarios via Monte Carlo simulations based on different levels of uncertainty or variability in loads and measurements. For each scenario, we ran the algorithm 20,000 times. The active p_j and the reactive q_j loads on each bus j are time varying. In order to simulate the normal behavior of the grid at each time t, $p_j(t)t$ and $q_j(t)$ are Gaussian random variables, i.e. $p_j(t) \sim \mathcal{N}(\bar{p}_j, \sigma_\ell^2), q_j(t) \sim \mathcal{N}(\bar{q}_j, \sigma_\ell^2)$, where $\bar{p}_j, \bar{q}_j$ are the nominal values that can be found in [15]. We explore the situations in which loads can vary up to 50% of their nominal value, by setting $3\sigma_\ell = 0, 0.1, 0.2, 0.3, 0.4, 0.5$. This choice is informed by [16], which presents an study on loads historical time series analysis. It shows that load estimations based on metering data typically have $30\% - 50\%$ uncertainty.

Each simulation run is as follows: 1) randomly choose an initial topology, 2) choose the switch that is going to change its status leading to the second topology, 3) perform the switch action at a certain time, 4) record the PMU measurement of voltage phasor at time t for each iteration, 5) compute the $\delta(t)$, 6) when we see a significant abrupt change (a spike) on the trend matrix norm, say at time T, we project $\delta(T)$ in the topology library $\mathcal{L}$ and finally 7) we identify the new topology by finding the maximum value.

Based on our studies, the magnitude of abrupt change in the time-series eigenvalues profile is related to the time window parameter $w$in the trend matrix. In this paper, we select w based on some heuristics through our simulations. In Figure 2, we can see how the choice of w influences the topology change detection. The topology change occurs at $t = 50$. If we choose $w = 1$ (black line), the spike is small and can be masked by other signal variations due to the load variability. With $w = 5$ (red line), the spike is clearly detectable. The same is true for $w = 10$ (blue line). Because a shorter time window of measurement records means less computational time for the algorithm, we choose the smaller $w = 5$ for the rest of our simulations. After detecting the time T of the topology

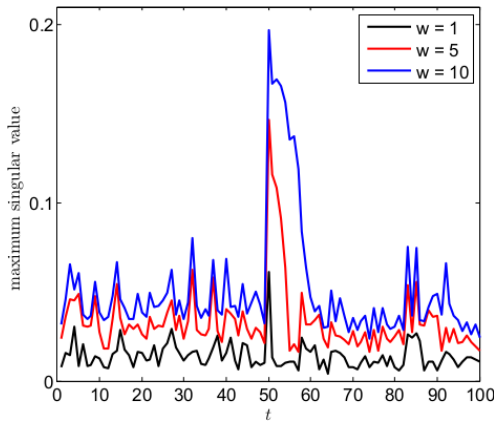

Figure 2. Maximum singular value trajectory of a Monte Carlo simulation. This is a particular realization where $3\sigma_\ell = 0.4$.

transition, the algorithm projects the trend vector on $\mathcal{L}$ and then decides which possible topology eigenvector is most similar to the eigenvector of the measurement trend vector.

To evaluate the performance of our algorithm, we examine its error rate in various scenarios, as shown in Figure 3. Each scenario is characterized by different values of measurement noise, and plotted against the uncertainty in the loads.
Scenario 1 *Noiseless measurements*: firstly we simulate our algorithm algorithm with ideal, noiseless measurements. The

results are depicted with the black line in Figure 3.

Scenario 2 *Measurements taken by μhigh-precision PMU devices*: we simulate our algorithm in a distribution network where we have the high-precision μPMU devices [17] on every bus. They are affected by two different types of noise, the voltage magnitude and the voltage phase angle. Let's assume that the voltage at bus j is given by u_j. The measured voltage magnitude is affected by the additive Gaussian noise $\epsilon_j \sim \mathcal{N}(0, \sigma_\epsilon |u_j|)$, while the measured voltage angle is affected by the additive Gaussian noise $\theta_j \sim \mathcal{N}(0, \sigma_\theta)$, where $\sigma_\epsilon = 0.05 \cdot 10^{-2}, \sigma_\theta = 0.01$. Therefore, the output of our PMU placed at bus j is

$$y_j = |u_j + \epsilon_j| e^{i(\angle u_j + \theta_j)} \tag{26}$$

The results are depicted with the red line in Figure 3.

Scenario 3 *Measurements taken by PMU devices with Total Vector Error (TVE) $\leq$ 0.005*: we simulate our algorithm in a network where PMU measurements are effected by Gaussian noise such that the Total Vector Error is less than 0.5 % (TVE = 0.005) based on the PMU manufacturer test information. It is also comply the IEEE standard C37.118.1-2011 for PMUs [18]. As a consequence, the output of our PMU placed at bus j is

$$y_j = u_j + e_j \tag{27}$$

where e_j is a complex number such that $|e_j| \leq TVE|u_j|$. The results are depicted with the green line in Figure 3.

Scenario 4 *Measurements taken by PMU devices with TVE $\leq$ 0.01*: we simulate our algorithm in a distribution network where PMU measurements are effected by Gaussian noise such that the Total Vector Error is less than 1 % (TVE = 0.01). It is also satisfying the IEEE standard C37.118.1-2011. The output of the PMU placed at bus j is again in the form given by (27), but this time with $|e_j| \leq TVE|u_j|$. The results are depicted with the blue line in Figure 3.

In Figure 3, notice that the black curve values for $\sigma_\ell = 0$ is zero, meaning that in the 20,000 runs the algorithm always succeeds. Therefore, we can see that in the steady-state condition and in the absence of noise, the algorithm is extremely efficient and robust for the 33-bus test case. It also overcomes the linearization from Proposition 2 and the initial Assumption 4. We can see that the red and the black lines converge and sometimes overlapping, meaning that the level of measurement noise assumed for the high-precision μPMU has a negligible impact compared to load variability. Finally we can see how the curves in Figure 3 have basically similar trajectory with different offset values. It shows that the load variability and the PMU accuracy are independently affecting accuracy of our topology detection algorithm, where the trajectory of the algorithm error is based on the load variability and its offset depends on the PMU device accuracy. More accurate PMUs leads to more accurate topology detection. In this paper, we assumed having PMUs on all buses. In future work, we will study the number of PMU devices and their placement impacts on the topology detection algorithm on a larger distribution network test bed.

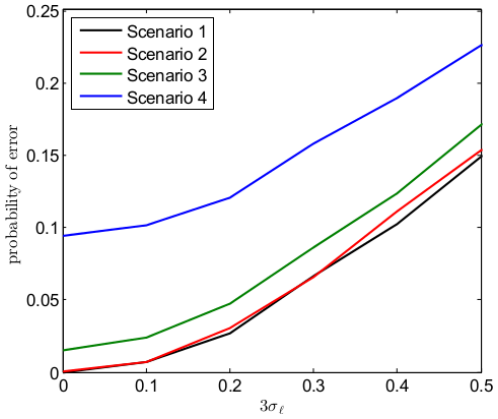

Figure 3. Error probability computed after the Monte Carlo simulations.

REFERENCES

[1] A. Monticelli, "Electric power system state estimation," *Proceedings of the IEEE*, vol. 88, no. 2, pp. 262–282, 2000.

[2] C. Lueken, P. M. Carvalho, and J. Apt, "Distribution grid reconfiguration reduces power losses and helps integrate renewables," *Energy Policy*, vol. 48, no. 0, pp. 260 – 273, 2012, special Section: Frontiers of Sustainability. [Online]. Available: http://www.sciencedirect.com/science/article/pii/S0301421512004351

[3] S. Bolognani, G. Cavraro, R. Carli, and S. Zampieri, "A distributed feedback control strategy for optimal reactive power flow with voltage constraints," *arXiv preprint arXiv:1303.7173*, 2013.

[4] "Chapter 34 - every moment counts: Synchrophasors for distribution networks with variable resources," in *Renewable Energy Integration*, L. E. Jones, Ed. Boston: Academic Press, 2014, pp. 429–438.

[5] G. N. Korres and N. M. Manousakis, "A state estimation algorithm for monitoring topology changes in distribution systems," in *Power and Energy Society General Meeting, 2012 IEEE*. IEEE, 2012, pp. 1–8.

[6] Y. Sharon, A. M. Annaswamy, A. L. Motto, and A. Chakraborty, "Topology identification in distribution network with limited measurements," in *Innovative Smart Grid Technologies (ISGT), 2012 IEEE PES*. IEEE, 2012, pp. 1–6.

[7] M. Ciobotaru, R. Teodorescu, and F. Blaabjerg, "On-line grid impedance estimation based on harmonic injection for grid-connected pv inverter," in *Industrial Electronics, 2007. ISIE 2007. IEEE International Symposium on*, June 2007, pp. 2437–2442.

[8] M. Liserre, F. Blaabjerg, and R. Teodorescu, "Grid impedance estimation via excitation of lcl -filter resonance," *Industry Applications, IEEE Transactions on*, vol. 43, no. 5, pp. 1401–1407, Sept 2007.

[9] A. von Meier, D. Culler, A. McEachern, and R. Arghandeh, "Micro-synchrophasors for distribution systems," in *Innovative Smart Grid Technologies Conference (ISGT), 2014 IEEE PES*, Feb 2014.

[10] S. Bolognani and S. Zampieri, "A distributed control strategy for reactive power compensation in smart microgrids," *IEEE Trans. on Automatic Control*, vol. 58, no. 11, November 2013.

[11] L. Schenato, G. Barchi, D. Macii, R. Arghandeh, K. Poolla, and A. Von Meier, "Bayesian linear state estimation using smart meters and pmus measurements in distribution grids," in *IEEE International Conference on Smart Grid Communications 2014*. IEEE, 2014.

[12] G. Cavraro, R. Carli, and S. Zampieri, "A distributed control algorithm for the minimization of the power generation cost in smart micro-grid," in *Conference on Decision and Control (CDC14)*, 2014.

[13] K. S. Miller, "On the inverse of the sum of matrices," *Mathematics Magazine*, pp. 67–72, 1981.

[14] B. M. Sanandaji, E. Bitar, K. Poolla, and T. L. Vincent, "An abrupt change detection heuristic with applications to cyber data attacks on power systems," *arXiv preprint arXiv:1404.1978*, 2014.

[15] R. Parasher, "Load flow analysis of radial distribution network using linear data structure," *arXiv preprint arXiv:1403.4702*, 2014.

[16] R. Sevlian and R. Rajagopal, "Short term electricity load forecasting on varying levels of aggregation," *arXiv preprint arXiv:1404.0058*, 2014.

[17] "Pqube 3, new low cost, high-precision power quality, energy and environment monitoring," in *Power Standard Lab. Inc. (PSL),http://www.powerstandards.com/*.

[18] "Ieee standard for synchrophasor measurements for power systems," *IEEE Std C37.118.1-2011 (Revision of IEEE Std C37.118-2005)*, pp. 1–61, Dec 2011.